TELKOMNIKA, Vol. 13, No. 4, December 2015, pp. 1127~1132
ISSN: 1693-6930, accredited A by DIKTI, Decree No: 58/DIKTI/Kep/2013
DOI: 10.12928/TELKOMNIKA.v13i4.1818

Research on Silicon-based Planar Spiral Inductance Coil Based on MEMS

Gang Li*[1], Xiaofeng Zhao[2], Dianzhong Wen*[3], Yang Yu[4]
Key Laboratory of Electronics Engineering, College of Heilongjiang Province, Heilongjiang University
No.74 of Xufu Road, Nangang district, Haerbin, Heilongjiang Province, China, +86-451-86609073
*Corresponding author, e-mail: ligang@hlju.edu.cn[1], zhaoxiaofeng@hlju.edu.cn[1],
wendianzhong@hlju.edu.cn[3], 1085562584@qq.com[4]

Abstract

This paper describes a kind of silicon-based plane spiral inductance coil, whose layout size and fabrication technology process are given. The production of inductance coil adopts the method of an internal down-lead produced by ohm contact electrode which is formed by heavily boron- diffused and the Al evaporated on the surface of N-type high resistivity silicon wafer. Processing the silicon cup on The back of the silicon wafer using MEMS technology, on the basis of thickness reduction of the inductance coil substrate, the porous array substrate of about 5μm thickness is obtained by laser drilling on the underside of the silicon cup, which reduces the vortex of substrate, and greatly improves the Q value of inductance coil. Analyze the effects of series resistance of the coil and metal layer thickness on the Q value in the condition of low frequency and high frequency, and Ansys software is used to simulate the inductance coil current density and magnetic induction intensity, to determine the optimum substrate thickness of inductance coil. The silicon-based plane spiralind inductance coil has the advantages of simple manufacturing process and is compatible with IC technology, compared with other manufacturing method, so it has a wide application prospect.

Keywords: *MEMS; silicon-based planar spiral inductance coil; Ansys; Q value*

1. Introduction

Silicon-based planar spiral inductance coil, as a kind of important passive components, has been widely applied to electronic technology [1]. Compared with other materials, the metallic inductance coil manufactured on silicon substrate requires difficult process[2-5], but that is compatible with the integrated circuit technology, so silicon-based planar spiral inductance coil is still the first choice for RFIC [6-8].

At present, some inductance coil production process is complex and high cost, which is not in conformity with the large scale integrated circuit development requirements of the high integration and low cost [9-11]. How to simplify the electromagnetic excitation of the resonant sensor production process, reduce the cost and keep high quality has become the key to the development of the technology.

In this paper, by using the planar spiral inductor model and analyzing the effects of series resistance of the coil and metal layer thickness on the Q value in the condition of low frequency and high frequency, a new method of manufacturing inductance coil is presented, which is an internal down-lead produced by ohm contact electrode formed by heavily boron-diffused and the Al evaporated on the back of silicon cup using MEMS technology, and the porous array substrate is obtained by laser drilling on the underside of the silicon cup to reduce the inductance coil loss. The study shows that the porous array substrate of about 5μm thickness is obtained by laser drilling on the underside of the silicon cup, which reduces the vortex of substrate, and greatly improves the Q value of inductance coil.

Received April 3, 2015; Revised July 22, 2015; Accepted August 12, 2015

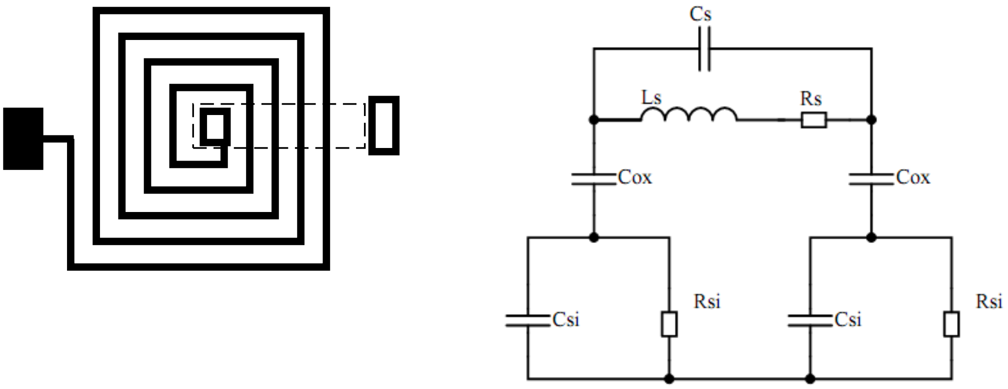

(a)

(b)

Figure 1. The model of silicon-based planar spiral inductance coil.
(a) Simple photo of inductance coil (b) Equivalent circuit of inductance coil

In Figure 1-(a), the inductance coil is manufactured on <100> orientation of monocrystalline silicon chip, which is N-type with high resistance and double-sided polishing. On the surface of silicon chip, we manufacture an inductance coil adopting the method of an internal down-lead produced by ohm contact electrode which is formed by heavily boron-diffused and the Al evaporated. When an alternating current is applied to the inductance coil, an alternating magnetic field will be generated.

Figure 1-(b) shows the equivalent circuit of plane spiral inductance coil, in which self-inductance value is L_s, resistance value is R_s, and C_s is capacitance between inductance coil wire, C_{ox} is capacitance between inductance coil and substrate, C_{si} and R_{si} are leakage capacitance and leakage resistance respectively, Q value expression is:

$$Q=\frac{wL_s}{R_s}\cdot\frac{R_p}{R_p+\left[\left(wL_s/R_s\right)^2+1\right]R_s}\cdot\left[1-\left(C_s+C_p\right)\left({R_s^2}/{L_s}+wL_s\right)\right] \tag{1}$$

Where R_p and C_p are given in equation (2) and (3):

$$R_p=\frac{1}{w^2C_{ox}^2R_{si}}+\frac{R_{si}\left(C_{ox}+C_{si}\right)^2}{C_{ox}^2} \tag{2}$$

$$C_p=C_{ox}\frac{1+w^2\left(C_{ox}+C_{si}\right)C_{si}R_{si}^2}{1+w^2\left(C_{ox}+C_{si}\right)^2R_{si}^2} \tag{3}$$

Resonant frequency of the inductance coil is given by

$$f=\frac{1}{2\pi}\sqrt{\frac{1}{L_s\left(C_p+C_s\right)}-\left(\frac{R_s}{L_s}\right)^2} \tag{4}$$

It can be seen from the analytical expressions is that the major factors causing the decrease of Q values are ohmic loss of coil, energy loss in the silicon substrate and loss resulted from the peak electric field power caused by parasitic capacitance increase with the frequency.

2.The Simulation and Calculation Methods

We use ANSYS software to make the simulation of the electromagnetic field generated by the inductance coil. Figure 2 and Figure 3 display the current density vector and magnetic induction intensity vector of static analysis when DC current is 10 mA. According to the magnetic field superposition principle, the total magnetic induction intensity is the magnetic induction intensity of x, y, z three directions overlay, the maximum magnetic induction intensity distribution in the inner coil. When alternating current of dynamic analysis is 10+10i mA, frequency of 100Hz, the alternating magnetic induction intensity simulated images of inductance coil in the air is shown in Figure 4. Figure 5 is the stress distribution of inductance coil substrate.

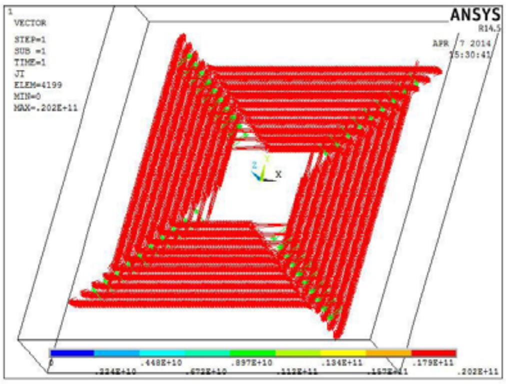

Figure 2. The picture of current density vector

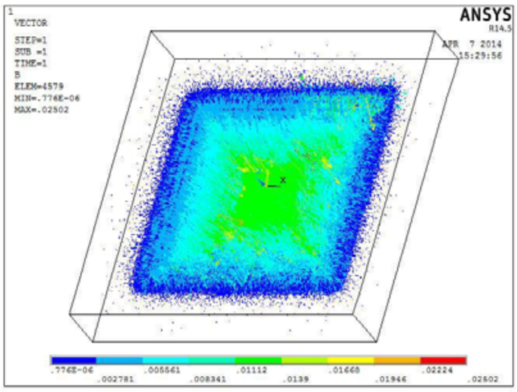

Figure 3. The picture of magnetic induction intensity vector

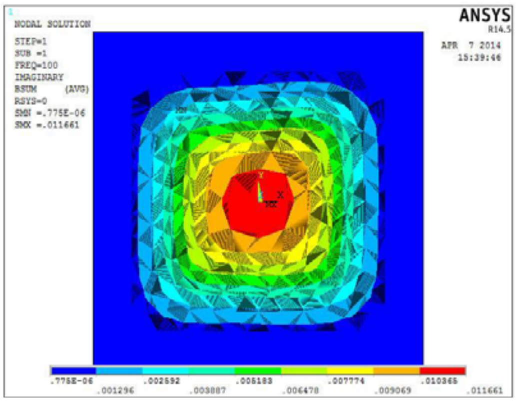

Figure 4. The picture of magnetic induction intensity

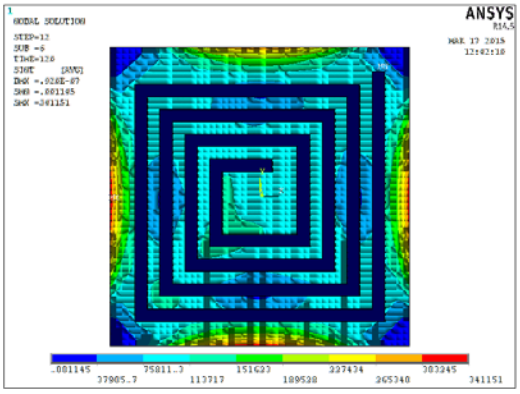

Figure 5. The stress distribution of inductance coil substrate

The inductance theoretical value is calculated by the Greenhouse method. The basic idea is to divide the rectangular coil into a series of wire segments, calculate self-inductance of each wire respectively and the mutual inductance between the two wires, and finally sum up all the self-inductance and mutual inductance of the wire section. Because of a large amount of computation, we wrote MATLAB program based on the size of the inductance coil to calculate the theoretical value of inductance coil according to its size by using the Greenhouse formula and get the inductance coil measured value.

3. Design and Manufacture of Inductance Coil

We adopt MEMS surface processing technology to design the inductance coil in this paper. The number of turns of the coil is 34, width of the coil conductor is 10 μm, and the coil conductor spacing is 10 μm. The fabrication technology process of the inductance coil is illustrated in Figure 6. Figure 7 is inductance coil sample photo.

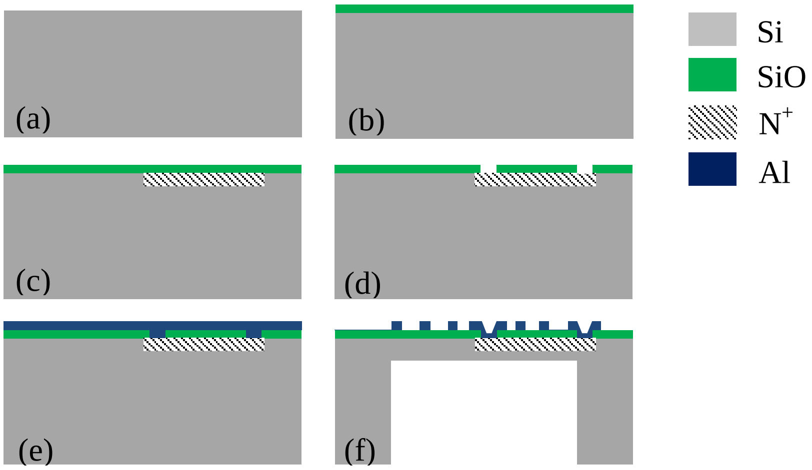

Figure 6. The fabrication technology process of inductance coil
(a) Silicon wafer cleaning; (b) Surface oxidation; (c) Boron diffusion; (d) Lithography conductor hole; (e) Vapor aluminized film; (f) Etching aluminized film to form inductance coil

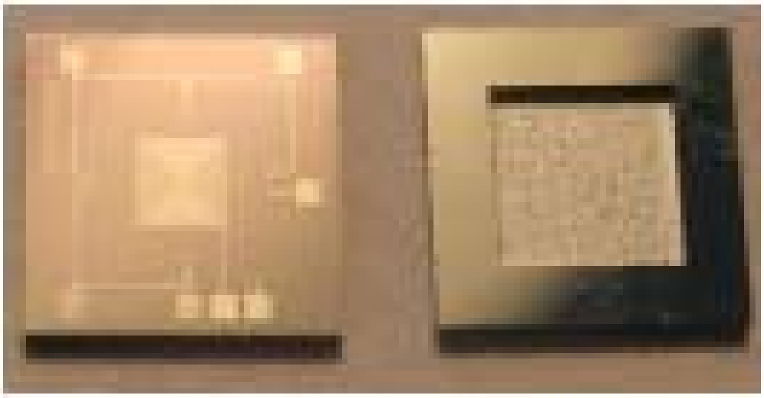

Figure 7. The photo of inductance coil sample

4. Experimental Results and Discussion

We get the inductance coil measured values and Q values in test condition of different frequencies by using precision LCR meter (TH2819A). The results of comparison between inductance coil theoretical value and the measured values are shown in Table 1. As can be seen from the Table, the measured value reached more than 22 μH, but the error is relatively large compared with the theoretical value. It is mainly due to ignorance of the internal down-lead, structure size of contact electrode, process conditions and precision of measuring instrument in the theoretical calculation.

Table 1. The comparison between the inductance theoretical value and the measured values of the coil

Frequency (KHz)	1	10	100	150	200
Measured Value(μH)	25.6646	25.0882	23.4840	23.1228	22.8745
Theoretical Value(μH)			47.26		
Error	45.70%	46.92%	50.31%	51.08%	51.60%

Figure 8 reflects Q values of the inductance coil change with frequencies. As is shown in the figure, Q values in less than 90 KHz range increase with the increase of frequency, but at more than 90 KHz, Q values decrease with the increase of frequency. This indicates that, in the high frequency, the energy loss in the silicon substrate increases with the frequency increased, resulting in the decrease of Q values.

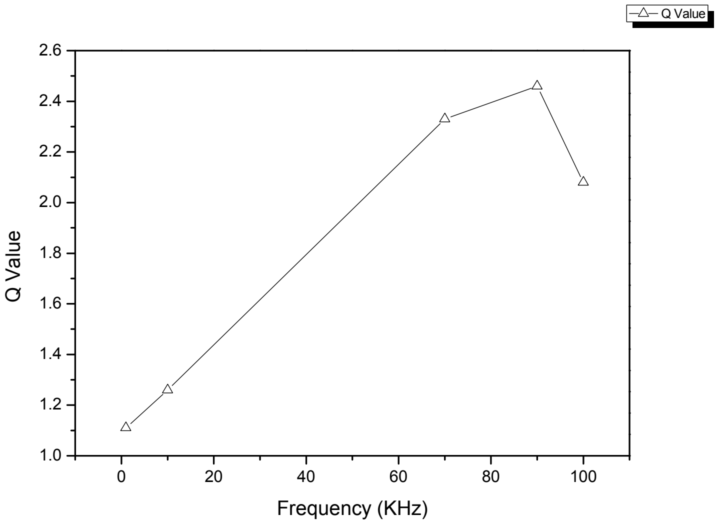

Figure 8. The Q value curve of different frequencies

5. Conclusion

The inductance coil designed in this paper acts as the driving element of electromagnetic excitation resonant sensor, and the magnitude of magnetic field generated by coil is the decisive factor of drive capability. We adopted N-type high resistivity silicon wafer whose resistivity is 100Ω·cm to produce an inductance coil of 34 turns, and obtain a larger inductance value. By the magnetic inductance energy formula $W=LI^2/2$, large inductance values can generate high magnetic field, causing the silicon membrane vibration.

At the same time, to reduce the thickness of porous array silicon membrane at the bottom of inductance coil to 5um, which can make the eddy current of substrate greatly reduce, playing an important role in inhibition of eddy current effect under high frequency. Through experimental demonstration, the inductance coil we design and manufacture in this paper is able to meet requirements of silicon micro pump, and has broad application prospects in microelectronics and micro system.

References

[1] Wen Dianzhong. Sensitivity Analysis of Junction Field Effect-Pressure Halltron. *Review of Scientific Instrument*. 1995; 66 (1): 251-255.

[2] Zhao Xiaofeng, Wen Dianzhong, Zhuang Cuicui, et al. Fabrication and Characteristics of the Magnetic Field Sensors Based on Nano-Polysilicon Thin-Film Transistors. *Journal of Semiconductors*. 2013; 34(3):036001(1-6).

[3] Zhao Xiaofeng, Wen Dianzhong, Li Gang. Fabrication and characteristics of the nc-Si/c-Si heterojunction MOSFETs pressure sensor. *Sensors*. 2012; 12(5): 6369-6379.

[4] Yoon JB, Choi YS, Kim B, et.al. CMOS Compatible Surface-Micromachined Suspended-Spiral Inductors for Multi-GHz Silicon RFICs. *IEEE Electron Device Letters*. 2002; 23(10): 591-593.

[5] Gradolph, Friedberger, Muller, et.al. Environments on piezoresistive pressure sensorImpact of high-g and high vibration performance. *Sensors and Actuators. A, Physical*. 2009; 150(1): 69-77.

[6] Jiang Qi-feng Li Zheng-Fang. Modeling and Analysis of Spiral Inductors for Si-Based RFIC’s. *Acta Electronic Sinica*. 2002; 30(8): 1119-1121.

[7] Mengran Liu, Guojun Zhang, Zeming Jian, et.al. Design of Array MEMS Vector Vibration Sensor in the Location of Pipeline Internal Inspector. *TELKOMNIKA Indonesian Journal of Electrical Engineering*. 2014; 12(9): 6651- 6657.

[8] Zhang Zhi-yong, Hai Chao-He. High Q-Factor On-chip Spiral Inductors for Bulk Silicon CMOS RF IC’S. *Microelectronics*. 2003; 33(1): 15-18.

[9] Waugh WH, Gallacher BJ, Burdess JS. A High-Sensitivity Resonant Sensor Realized Through the Exploitation of Nonlinear Dynamic Behavior. *Mess Sci Technol*. 2011; 22(10): 105-202.

[10] Achmad Widodo, Latief Rozaqi, Ismoyo Haryanto, et.al. Development of Wireless Smart Sensor for Structure and Machine Monitoring. *TELKOMNIKA Telecommunication Computing Electronics and Control*. 2013; 11(2): 417-424.

[11] Peng Guanbin, Liu Jingquan, Wand Longfei, et.al. Circuit Design of an Implantable MEMS Pressure Sensor System. *Nanotechnology and Precision Engineering*. 2013; 11(1): 90–95.